Thermochimica Acta, 179 (1991) 313–322
Elsevier Science Publishers B.V., Amsterdam

THERMAL AND SPECTRAL STUDIES OF 1-(2′-HYDROXYBENZYL)-2-(2′-HYDROXYPHENYL)BENZIMIDAZOLE COMPLEXES OF IRON(III), COBALT(II), NICKEL(II) AND COPPER(II)

K.K. MOHAMMED YUSUFF * and R. SREEKALA

Department of Applied Chemistry, Cochin University of Science and Technology, Cochin-682 022 (India)

(Received 19 June 1990; in revised form 6 August 1990)

ABSTRACT

Novel Fe(III), Co(II), Ni(II) and Cu(II) complexes of 1-(2′-hydroxybenzyl)-2-(2′-hydroxyphenyl)benzimidazole (L) have been synthesized and characterized. The general formula for the Co(II), Ni(II) and Cu(II) complexes is $[ML(OH)(H_2O)]\cdot H_2O$, and for the iron(III) complex, $[FeL(OH)_2(H_2O)_2]\cdot H_2O$. Octahedral and square planar structures have been assigned for the iron(III) and copper(II) complexes respectively, while the cobalt(II) and nickel(II) complexes have tetrahedral structures. The bonding of the ligand is through the N-3 atom and one of the phenolic OH groups. The complexes were subjected to a systematic TG/DTG/DTA analysis. The decomposition process consists of two stages for the nickel(II) complex and three stages for the other complexes. Kinetic parameters were evaluated for each of these stages using the Coats–Redfern equation. The rate of decomposition at the final stage seems to have a bearing on the oxygen chemisorption capabilities of the metal oxides formed during this stage.

INTRODUCTION

In recent years there has been considerable interest in complexes formed by imidazole, benzimidazole and related ligands because such donors are common components of some important biological molecules [1–3]. For example, 5,6-dimethylbenzimidazole supplies one of the five nitrogen atoms coordinated to cobalt in vitamin B_{12} [4]. Furthermore, benzimidazoles have been reported to possess a wide range of biological activities, including antibacterial, antifungal and antiviral [5–8].

The synthesis and characterization of 1-(2′-hydroxybenzyl)-2-(2′-hydroxyphenyl)benzimidazole (HBHPBI) complexes of copper(II), iron(III), iron(II) and cobalt(II) have been reported earlier [9,10]. In these complexes, intramolecularly hydrogen-bonded phenolic OH groups of the ligand do not

---

* Author to whom correspondence should be addressed.

0040-6031/91/$03.50

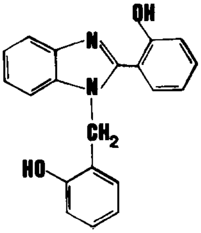

Fig. 1. Structure of HBHPBI.

take part in complexation. But using a different synthetic procedure, we have prepared novel Fe(III), Co(II), Ni(II) and Cu(II) complexes of the ligand, HBHPBI (Fig. 1), in which one of its phenolic oxygen atoms is coordinated to the metal atom. Although a large number of transition metal complexes containing imidazoles and benzimidazoles as ligands have been studied, the kinetic aspects of the thermal decomposition of these compounds have very rarely been studied [11]. Here we report our investigations on the synthesis, and the spectral, magnetic and thermal decomposition kinetic studies of these HBHPBI complexes.

EXPERIMENTAL

Synthesis of the ligand

The ligand HBHPBI was prepared according to the procedure given in the literature [12].

Synthesis of the complexes

The ligand HBHPBI (0.01 mole) was dissolved in 80 ml of 1% NaOH solution. The solution was neutralized with a few drops of dilute acetic acid, and to this was added 0.005 mole of metal chloride solution in 25 ml of water. The complex separated out and was filtered, washed several times with water and dried over anhydrous calcium chloride.

Analytical methods

Iron, cobalt, nickel and copper analyses were carried out using standard procedures [13]. Microanalyses for carbon, hydrogen and nitrogen were performed on a Perkin-Elmer 2400 CHN elemental analyser. Magnetic susceptibilities were measured at 300 ± 2 K using an EG&G PARC Model 155 vibrating sample magnetometer. Infrared spectra of the ligand and the complexes in the region 600–4000 cm^{-1} were taken both in Nujol mull and as KBr discs, and in the region 200–600 cm^{-1} in polyethylene matrix, using a Perkin–Elmer 983 infrared spectrophotometer. Solid state electronic spectra in the region 200–2000 nm were recorded with a Hitachi U-3410 spectrophotometer using the mull technique [14]. Thermal studies were carried out with a Ulvac Sinku–Riko TA-1500 thermal analyser at a heating rate of 10 °C min^{-1} in an air atmosphere using a platinum crucible. The mass of the samples used was in the range 5–8 mg. The evaluation of the kinetic parameters, i.e. order n, energy of activation E_a, entropy of activation ΔS, and pre-exponential factor A, using the Coats–Redfern equation [15] was based on a computer program which was developed for use on a Busybee PC/XT computer (HCL Ltd.).

RESULTS AND DISCUSSION

All the complexes are crystalline, non-hygroscopic, coloured substances, which are stable to air oxidation. The complexes are slightly soluble in methanol, ethanol and acetone, and are moderately soluble in DMF and DMSO. The analytical data (Table 1) show that the complexes have the general formula $[ML(OH)(H_2O)] \cdot H_2O$ for the Co(II), Ni(II) and Cu(II) complexes, and $[FeL(OH)_2(H_2O)_2] \cdot H_2O$ for the Fe(III) complex (where L = HBHPBI).

Magnetic measurement studies

Magnetic moment values of the complexes are presented in Table 2. The iron(III) complex has a magnetic moment of 5.92 B.M., which suggests a high spin octahedral complex [16]. The magnetic moment value of 4.3 B.M. for the Co(II) complex suggests a tetrahedral structure [17]. For the Ni(II)

TABLE 1

Analytical data

Substance	Colour	Carbon found (%) (calc.)	Hydrogen found (%) (calc.)	Nitrogen found (%) (calc.)	Metal found (%) (calc.)
Fe complex	Reddish brown	52.06 (51.85)	5.00 (4.75)	6.09 (6.05)	12.10 (12.06)
Co complex	Grey	55.73 (55.64)	4.51 (4.41)	6.62 (6.50)	13.70 (13.68)
Ni complex	Light green	55.86 (55.72)	4.71 (4.41)	6.54 (6.50)	13.68 (13.63)
Cu complex	Green	55.61 (55.10)	4.51 (4.36)	6.48 (6.43)	14.70 (14.59)

TABLE 2

Magnetic moment and electronic spectral data

Substance	Magnetic moment	Absorption maxima (cm^{-1})	Tentative assignments
Fe complex	5.92	34800	Transitions within the ligand
		30000	Charge transfer transitions
		21200	Forbidden d–d transitions
Co complex	4.30	35000	Transitions within the ligand
		25000	Charge transfer transitions
		16180	$^4A_2 \rightarrow {}^4T_1(P)$
		9300	$^4A_2 \rightarrow {}^4T_1(F)$
Ni complex	3.80	40000	Transitions within the ligand
		26100	Charge transfer transitions
		14500	$^3T_1(F) \rightarrow {}^3T_1(P)$
		8730	$^3T_1(F) \rightarrow {}^3A_2(F)$
Cu complex	1.73	34000	Transitions within the ligand
		27450	Charge transfer transitions
		21000	$^2B_{1g} \rightarrow {}^2A_{1g}$
		15300	$^2B_{1g} \rightarrow {}^2B_{2g}$
		12500	$^2B_{1g} \rightarrow {}^2E_{1g}$

complex the magnetic moment value (3.8 B.M.) also suggests a tetrahedral structure [18]. The magnetic moments of simple Cu(II) complexes are generally in the range 1.73–2.20 B.M. regardless of stereochemistry [19]. The present Cu(II) complex has a magnetic moment value of 1.73 B.M. This slightly lower magnetic moment value suggests that the complex does not have a tetrahedral structure [19]. Therefore, a square planar structure can be assumed for this complex.

Electronic spectra

Because of the greater oxidizing power of Fe(III), ligand to metal charge transfer bands often obscure the very low intensity d–d absorption. The electronic spectrum of the Fe(III) complex shows a broad absorption band with a maximum around 21 000 cm^{-1} corresponding to a combination of $^6A_{1g} \rightarrow {}^4T_{1g}$, $^6A_{1g} \rightarrow {}^4T_{2g}$, and $^6A_{1g} \rightarrow {}^4E_g$ forbidden transitions in the octahedral symmetry [20].

The Co(II) complex exhibits an absorption band at around 16 180 cm^{-1}, which can be assigned to $^4A_2 \rightarrow {}^4T_1(P)$ electronic transition. It also exhibits a broad absorption band around 9300 cm^{-1} due to the $^4A_2 \rightarrow {}^4T_1(F)$ transition. The transition $^4A_2 \rightarrow {}^4T_2$ is not observed in the spectrum of the present complex. In most instances it is seldom observed as it is inherently weak due to an orbital selection rule [21]. Thus, the electronic spectrum of the cobalt(II) complex supports the magnetic moment value in suggesting a tetrahedral structure for the complex. The nickel(II) complex also displays absorption bands indicative of tetrahedral geometry. It exhibits two bands, one at 14500 cm^{-1} and the other at 8730 cm^{-1}, which could be assigned to the $^3T_1(F) \rightarrow {}^3T_1(P)$ and $^3T_1(F) \rightarrow {}^3A_2(F)$ transitions respectively [21].

It is difficult to distinguish between a square planar and tetrahedral geometry for copper(II) ion. However, the electronic spectrum of the present Cu(II) complex shows a broad absorption band with shoulders at 12500, 15300 and 21000 cm^{-1}. Assuming a square planar geometry, these could be assigned to $^2B_{1g} \rightarrow {}^2A_{1g}$, $^2B_{1g} \rightarrow {}^2B_{2g}$, and $^2B_{1g} \rightarrow {}^2E_{1g}$ transitions respectively [22].

Furthermore, all the complexes exhibit a broad absorption band in the region 25000–30000 cm^{-1} which might be due to charge transfer transitions. Transitions within the ligand occur in the region 34000–40000 cm^{-1}.

Infrared spectra

All the complexes exhibit a very broad band in the 3100–3500 cm^{-1} region due to O–H stretching vibrations [23]. In addition, a double hump at around 3010 cm^{-1} and a sharp band at 840 cm^{-1} are seen in the spectra of the complexes due to coordinated water molecules [24].

The band of medium intensity at 1500 cm^{-1} in the spectrum of the free HBHPBI ligand may be attributed to the C–N stretching vibrations. In the case of the present complexes this band shifts to 1490 cm^{-1}. The shifting of this band to a lower frequency was observed by earlier workers and has been interpreted as being due to the coordination of the N-3 atom of benzimidazole to the metal atom [25].

In the spectra of free HBHPBI and its complexes, there is a band at around 1280 cm^{-1} which is assigned to the ν_{C-O} stretching vibration of the phenolic group [26]. The phenolic C–O bands of the uncoordinated ligand shift to higher frequencies during complex formation [27]. An additional band at 1310 cm^{-1} is found in the case of all the complexes. The presence of this band and the retention of the 1280 cm^{-1} band in the spectra of all the present complexes suggest that only one of the phenolic oxygen atoms is coordinated to the metal atom. Furthermore, all the complexes exhibit M–O–H bending modes at around 1120 cm^{-1}. A band at around 320 cm^{-1} due to ν_{M-N} and another band around 420 cm^{-1} due to ν_{M-O} are also observed in all cases [28].

Thermal behaviour

The TG/DTG/DTA curves for all the complexes are shown in Fig. 2. Thermoanalytical data for the complexes are presented in Table 3. The

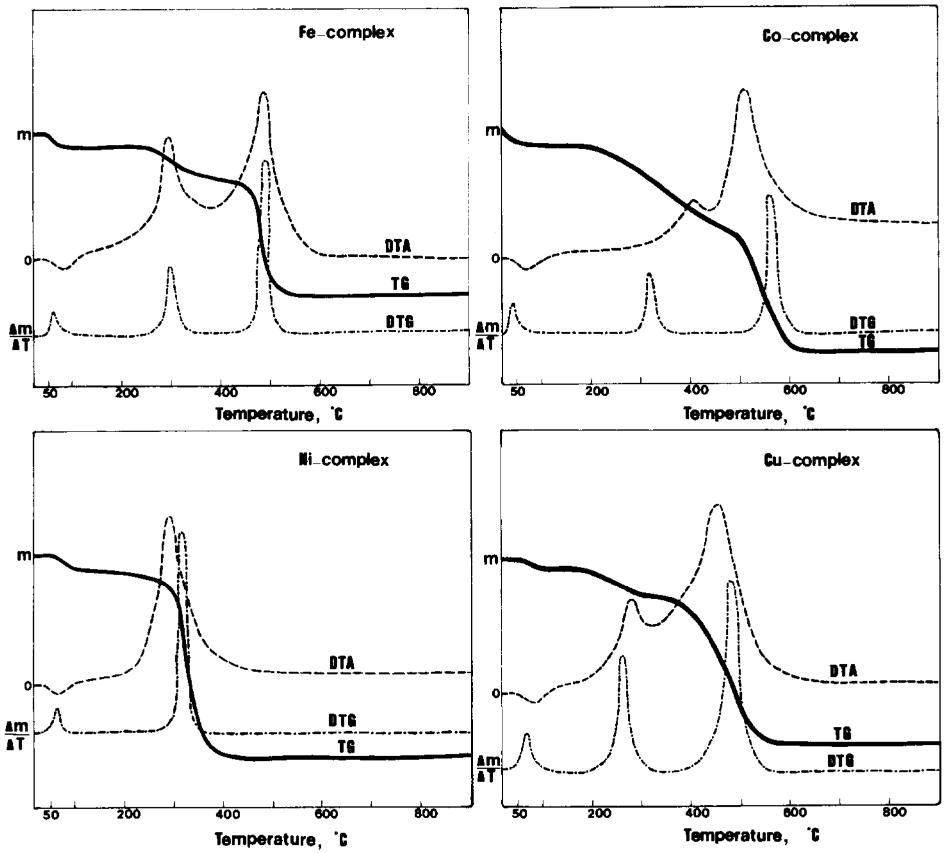

Fig. 2. TG, DTG, and DTA curves of complexes.

percentage mass loss and the probable compositions of the expelled groups and the residues are also given in this table.

The DTG curves show three peaks for Fe(III), Co(II) and Cu(II) complexes and two peaks for the Ni(II) complex. All these DTG peaks have their parallel DTA peaks. It is evident from the DTA curves that the loss of lattice water in all cases is an endothermic process, while the subsequent reactions appear to be exothermic in nature. The exothermicity in these cases is due to the concomitant decomposition and oxidation processes taking place at these stages. The high heat of decomposition released during the oxidation process might have masked the endothermicity of the decomposition reactions.

In all the complexes, the first decomposition stage begins at around 40 °C and is complete at 120 °C. The mass loss at this stage corresponds to the removal of one molecule of water. This water is not coordinated to the metal, as it is lost below 120 °C, and is probably lattice water. The evidence for lattice water is present in the IR spectra of these complexes which show a broad band in the region 3100–3500 cm^{-1}.

TABLE 3

Thermal decomposition data [a]

Substance	Peak temp. in DTA (°C)	Temp. range in DTA (°C)	Peak temp. in DTG (°C)	Temp. range in DTG (°C)	Stage	Loss found from TG (%) (calc.)	Probable composition of expelled group
Fe complex	80 endo(w)	50–110	65(w)	50– 95	I	4.20 (3.80)	H_2O
	295 exo (m)	220–370	300 (m)	260–340	II	15.22 (15.10)	2OH and $2H_2O$
	485 exo(s)	400–550	490 (s)	460–540	III	67.10 (68.90)	L
Co complex	70 endo(w)	40–120	40(w)	30– 80	I	4.50 (4.10)	H_2O
	410 exo (m)	300–440	320(m)	290–360	II	32.50 (33.10)	OH, H_2O and 0.3L
	510 exo(s)	450–620	560(s)	520–610	III	48.50 (49.40)	0.7L
Ni complex	65 endo(w)	30–100	60(w)	40– 75	I	4.60 (4.17)	H_2O
	300 exo(s)	260–400	320(s)	280–350	II	81.81 (82.23)	OH, H_2O and L
Cu complex	80 endo(w)	50–120	70(w)	50– 90	I	4.50 (4.13)	H_2O
	280 exo(m)	170–310	265(m)	200–290	II	10.48 (8.04)	OH and H_2O
	460 exo(s)	350–550	485(s)	400–550	III	69.45 (73.20)	L

[a] Abbreviations: s = strong, m = medium, w = weak, endo = endothermic, exo = exothermic, L = HBHPBI.

The first DTG peak is followed by a medium DTG peak in the case of the Fe(III), Co(II) and Cu(II) complexes, and a strong DTG peak in the case of the Ni(II) complex. The mass loss at this stage corresponds to the removal of coordinated water molecules and OH groups in the case of Fe(III) and Cu(II) complexes, and coordinated water molecules, OH groups and 0.3 HBHPBI molecule in the case of the Co(II) complex. The IR spectra of the residues after this stage showed the presence of HBHPBI ligand. For the Ni(II) complex, mass loss at this stage corresponds to the removal of a coordinated water molecule, an OH group and one HBHPBI molecule.

Except for the Ni(II) complex, all the complexes show one more strong DTG peak which corresponds to the removal of one HBHPBI molecule, in the case of the Fe(III) and Cu(II) complexes, and 0.7 HBHPBI molecule in the case of the Co(II) complex. In all cases, the residue after the final stage of decomposition was found to be the metal oxide.

TABLE 4

Kinetic data

Substance	Stage	Order(n)	E_a (kJ mol^{-1})	ΔS (kJ mol^{-1} K^{-1})	A (S^{-1})
Fe complex	I	0.23	34	−190	8.279×10^2
	II	1.06	79	−164	3.580×10^4
	III	1.91	406	269	1.806×10^{27}
Co complex	I	1.75	43	−149	1.086×10^5
	II	0.33	48	−223	0.281×10^2
	III	1.18	170	−91	2.955×10^8
Ni complex	I	0.38	23	−218	0.283×10^2
	II	1.83	148	−45	5.680×10^{10}
Cu complex	I	0.90	32	−239	2.381×10^2
	II	1.49	20	−288	0.105×10^0
	III	0.77	97	−172	1.729×10^4

Decomposition kinetics

There has been considerable discussion in the literature concerning the validity of kinetic data obtained by thermal analysis under non-isothermal conditions [29,30]. However, the method has certain advantages [31]. Several methods have been employed for the calculation of kinetic parameters from non-isothermal TG data. In the present case, the kinetic parameters n, E_a, ΔS and A, for all decomposition stages, have been calculated using the Coats–Redfern equation and are presented in Table 4. The order n of the reaction in these cases does not provide any meaningful information about the decomposition mechanism of the complexes. However, the parameters E_a and ΔS may be employed for the comparison of a given decomposition process for similar compounds [32]. In the present investigation, these values have been evaluated using the same equation for nearly the same experimental conditions (same heating rate, furnace atmosphere, sample weight etc.), and hence can be used conveniently for comparison purposes.

It can be seen from Table 4 that the order parameter for different decomposition stages is a decimal number. It is known from the literature that this order n need not be an integer [33,34]. The energy of activation for the decomposition of lattice-interacted water is in the range 23–44 kJ mol^{-1}, much lower than that for the coordinated water. These values are closer to the activation energy values for the dehydration reactions reported by earlier workers [35].

The E_a and ΔS values for the second stage of decomposition of all the complexes, except the Ni(II) complex, were found to be much lower than those for the third stage of decomposition. The lower value of E_a indicates an increased rate at this stage, and might be due to the catalytic effect of the metal complexes in the oxidation of the ligands and other decomposition products. The negative ΔS value indicates a more ordered activated state through the chemisorption of oxygen and other decomposition products [36]. For all catalysis reactions, chemisorption of the reactants is the prime requirement [37].

The E_a and ΔS values for the third stage of decomposition for the Fe(III), Co(II) and Cu(II) complexes were found to be much higher than those for the other stages, indicating that the rate of decomposition for this stage is lower than for the other stages. It is generally observed that step-wise formation constants decrease with an increase in the number of ligands attached to the metal ion [16]. It can therefore be expected that the rate of removal of the remaining ligands will be lower after the expulsion of one or two ligands.

For the Ni(II) complex, the second decomposition stage is the final stage, and the decomposition is complete at the lower temperature of 350 °C. For the other metal complexes, the decomposition is complete only above 540 °C. The faster decomposition for the Ni(II) complex at this stage might be due to the catalytic effect of nickel oxide formed during the decomposition. This is also indicated from the lower E_a value and the negative ΔS value for this complex at this stage. Oxygen adsorption is found to occur far more extensively on p-type oxides than on n-type oxides. NiO is known to be a p-type oxide, and hence works as a better catalyst for oxidation reactions [37].

Thus the decomposition at the final stage seems to have a bearing on the catalytic effect of the oxides formed at this stage. The lower value of E_a and the negative ΔS value for the Cu(II) complex suggests that the oxide formed might be p-type Cu_2O (this will ultimately be oxidized to CuO). The E_a value for the Co(II) complex is slightly higher than that for the Ni(II) complex. Here also, involvement of a p-type oxide, CoO, is indicated as the ΔS value is negative. However, for the Fe(III) complex, formation of n-type Fe_2O_3 is suspected at the final stage of decomposition, as the E_a and ΔS values are very much higher for this stage.

ACKNOWLEDGEMENTS

The authors are thankful to Professor K.L. Sebastian for developing the computer program for the evaluation of kinetic parameters. They are also thankful to RSIC, IIT, Madras for the instrumental facilities.

REFERENCES

1 M.N. Hughes, The Inorganic Chemistry of Biological Processes, Wiley, London, 1972.
2 G.L. Eichhorn (Ed.), Inorganic biochemistry, Elsevier, Amsterdam, 1973.

3 K.G. Strothkamp and S.J. Lippard, Acc. Chem. Res., 10 (1982) 318.
4 R.J. Sundberg and R.B. Martin, Chem. Rev., 74 (1974) 471.
5 S. Bahadur, A.K. Gorl and R.S. Varma, J. Indian Chem. Soc., 53 (1976) 1163.
6 V.M. Reddy, M.A.S. Chary and S.M. Reddy, Indian Drugs, 15 (1980) 7.
7 R.L. Thompson, J. Immunol., 55 (1947) 345.
8 W.R. Roderick, C.W. Nordeen, A.M. von Esdh and H.N. Appell, J. Med. Chem., 15 (1972) 655.
9 L.D. Prabhakar, K.M.M.S. Prakash and M.C. Chowdary, Inorg. Chim. Acta, 133 (1987) 233.
10 L.D. Prabhakar, K.M.M.S. Prakash and M.C. Chowdary, Synth. React. Inorg. Met. Org. Chem., 19 (1987) 937.
11 K.K.M. Yusuff and R. Sreekala, Thermochim. Acta, 159 (1990) 357.
12 N.V. Subba Rao and C.V. Ratnam, Proc. Indian Acad. Sci., 43A (1956) 174.
13 A.I. Vogel, A Text Book of Quantitative Inorganic Analysis, Longmans Green, London, 1968.
14 G. Dyer, J.G. Hartley and L.M. Venanzi, J. Chem. Soc., (1965) 1293.
15 A.W. Coats and J.P. Redfern, Nature, 68 (1964) 201.
16 S.A. Cotton and G. Wilkinson, Advanced Inorganic Chemistry, Wiley, New York, 4th edn., 1980.
17 M. Goodgame and F.A. Cotton, J. Am. Chem. Soc., 84 (1962) 1543.
18 M. Baral, B.K. Kanungo and B. Pradhan, J. Indian Chem. Soc., 63 (1986) 1018.
19 A. Earnshaw, Introduction to Magnetochemistry, Academic Press, New York, 1968.
20 S.A. Cotton, Coord. Chem. Rev., 8 (1972) 184.
21 A.B.P. Lever, Inorganic Electronic Spectroscopy, Elsevier, New York, 1968.
22 B.V. Patel, K. Desai and B.T. Thaker, Synth. React. Inorg. Met. Org. Chem., 19 (1989) 391.
23 J.R. Ferraro and W.R. Wacker, Inorg. Chem., 4 (1965) 1382.
24 I. Gamo, Bull. Chem. Soc. Jpn, 34 (1961) 760.
25 K.S. Bose and C.C. Patel, J. Inorg. Nucl. Chem., 32 (1970) 1141.
26 K. Nakanishi and P.H. Solomon, Infrared Absorption Spectroscopy, Holden–Day, San Francisco, 2nd edn., 1977.
27 T.M. Aminabhavi, N.S. Biradar, V.L. Roddabasanagoudar, W.E. Rudzinski and D.E. Hoffman, Inorg. Chim. Acta, 121 (1986) L45.
28 K. Nakamoto, Infrared Spectra of Inorganic and Coordination Compounds, Wiley New York, 2nd edn., 1970.
29 C.H. Bamford and C.F.H. Tipper, Comprehensive Chemical Kinetics, Vol. 22, Elsevier, Amsterdam, 1980.
30 P.M.D. Benoit, R.G. Ferrillo and A.H. Granzow, J. Therm. Anal., 30 (1985) 869.
31 W.W. Wendlandt, Thermal Methods of Analysis, Wiley, New York, 2nd edn., 1974.
32 G.N. Natu, S.B. Kulkarni and P.S. Dhar, J. Therm. Anal., 23 (1982) 101.
33 D. Blecic and Z.D. Zivkovic, Thermochim. Acta, 60 (1983) 68.
34 A.C. Norris, M.I. Pope and M. Selwood, Thermochim. Acta, 41 (1980) 357.
35 A. Srivastava, P. Singh, V.G. Gunjikar and A.P.B. Sinha, Thermochim. Acta, 86 (1985) 77.
36 P.M. Madhusudanan, K.K.M. Yusuff and C.G.R. Nair, J. Therm. Anal., 8 (1975) 31.
37 G.C. Bond, Heterogeneous Catalysis: Principles and Applications, Oxford University Press, London, 1974.